CSIRO PUBLISHING

www.publish.csiro.au/journals/ijwf *International Journal of Wildland Fire*, 2006, **15**, 179–186

Laboratory fire spread analysis using visual and infrared images

J. Ramiro Martínez-de Dios[A,C], *Jorge C. André*[B], *João C. Gonçalves*[B], *Begoña Ch. Arrue*[A], *Aníbal Ollero*[A] *and Domingos X. Viegas*[B]

[A]Grupo de Robótica, Visión y Control, Escuela Superior de Ingenieros, Universidad de Sevilla, Camino de los Descubrimientos, 41092 Sevilla, Spain.

[B]Departamento de Engenharia Mecânica, Universidade de Coimbra, Pinhal de Marrocos, 3030-201 Coimbra, Portugal.

[C]Corresponding author. Email: jdedios@cartuja.us.es

Abstract. This paper presents an experimental method using computer-based image processing techniques of visual and infrared movies of a propagating fire front, taken from one or more cameras, to supply the time evolutions of the fire front shape and position, flame inclination angle, height, and base width. As secondary outputs, it also provides the fire front rate of spread and a 3D graphical model of the fire front that can be rendered from any virtual view. The method is automatic and non-intrusive, has space–time resolution close to continuum and can be run in real-time or deferred modes. It is demonstrated in simple laboratory experiments in beds of pine needles set upon an inclinable burn table, with point and linear ignitions, but can be extended to open field situations.

Additional keywords: fire behavior; image processing techniques; laboratory experiments; sensor fusion.

Introduction

Visual and infrared cameras have been used to follow forest fire fronts and to determine the flame height, base depth, and inclination angle along the front (Britton *et al*. 1977; Clements 1983; Adkins 1995), and even to measure the velocity field in the convection column above the fire front (Clark *et al*. 1999; Zhou *et al*. 2003), and the radiation intensity and temperature fields in the flames (Den Breejen *et al*. 1998).

The goal of the present paper is to draw the attention of fire modelers to the potentialities of these types of techniques to measure specifically the geometrical properties of fire fronts. Particular techniques based on the automatic processing of images from visual and infrared cameras are described and demonstrated in laboratory experiments but can also be extended to open field conditions (Viegas *et al*. 2002).

Basic experimental set-up

The demonstration experiments mentioned below were carried out indoors, in a flat burn table of $1.6 \times 1.6\,m^2$, inclinable at an angle between 0° and 40°. The fuel bed was a statistically homogeneous layer of *Pinus pinaster* dead needles with load 1 kg/m^2 (dry weight) and moisture content around 12% (of dry weight). Fire tests with point and linear ignitions were performed.

Visual images are usually easy to interpret. Depending on the location and orientation of the camera relative to the fire front, they can be used to measure the flame height and inclination angle, and also to identify the fire front leading or rear edge when not occluded by flames or smoke. The visual camera used in the tests was a JAI2060 with 752×582 pixels and focal length of 8.5 mm.

Infrared cameras provide images of the radiation intensity field within the infrared range. The camera used in these experiments (Mitsubishi IR-M300E with 256×256 sensors and focal length of 25 mm) has spectral response in the mid-infrared (3–5 μm), with optimal sensitivity in the range of temperature 600–1000°C (Wien's Law; Hudson 1969). In this infrared band, the radiation intensity emitted by the embers at the fire base is considerably higher than that of the flames but the latter can still be seen (cf. Den Breejen *et al*. 1998), facilitating the interpretation of the image. Besides, the images are not occluded by smoke. In this way, infrared images permit the neat observation of the fire base, allowing the identification of the fire front leading and rear edges.

In the experiments, the cameras were placed at two view points (Figs 1 and 2): frontal view (*Camera 1*, visual [Fig. 2*c*,*f*] or infrared [Fig. 2*a*,*d*]), and lateral view (*Camera 2*, visual [Fig. 2*b*,*e*]). Depending on the experiment, some geometrical features of fire could be extracted from the images from only one camera (e.g. flame angle) or from several synchronized cameras (e.g. edges of the fire front).

10.1071/WF05004 1049-8001/06/020179

Image processing techniques

With the objective of measuring the slow evolution of geometrical features of the main fire-front, the images of each camera movie were sampled at 1 Hz and processed in real-time. Preliminary analyses with sampling frequencies of up to 25 Hz (PAL video standard) showed that, in all cases, the results for the fire features differed, on average, by less than ±0.1% from those obtained with the sampling frequency of 1 Hz.

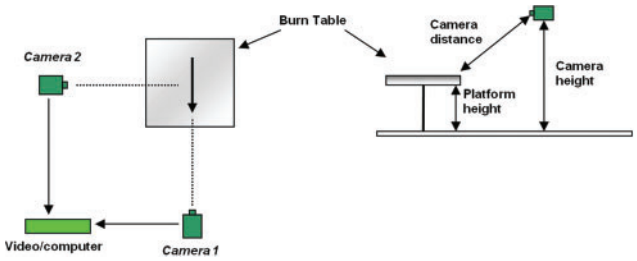

Fig. 1. General configuration of a laboratory experiment.

Basic enhancement of the image and fire contour detection

First, a median filter was applied to reduce the level of noise introduced in the images by the video transmission and capturing processes. Then, fire front was differentiated from the background with a threshold method. For visual images, the method of Ridler and Calvard (1978) allowed a fairly neat identification of the yellow region of the flames. Thermal and non-thermal infrared cameras were considered. For non-thermal infrared images, the method of Martínez-de Dios and Ollero (2002) was used to distinguish fire and background pixels. Thermal infrared cameras include software that converts the primary measures of radiation into

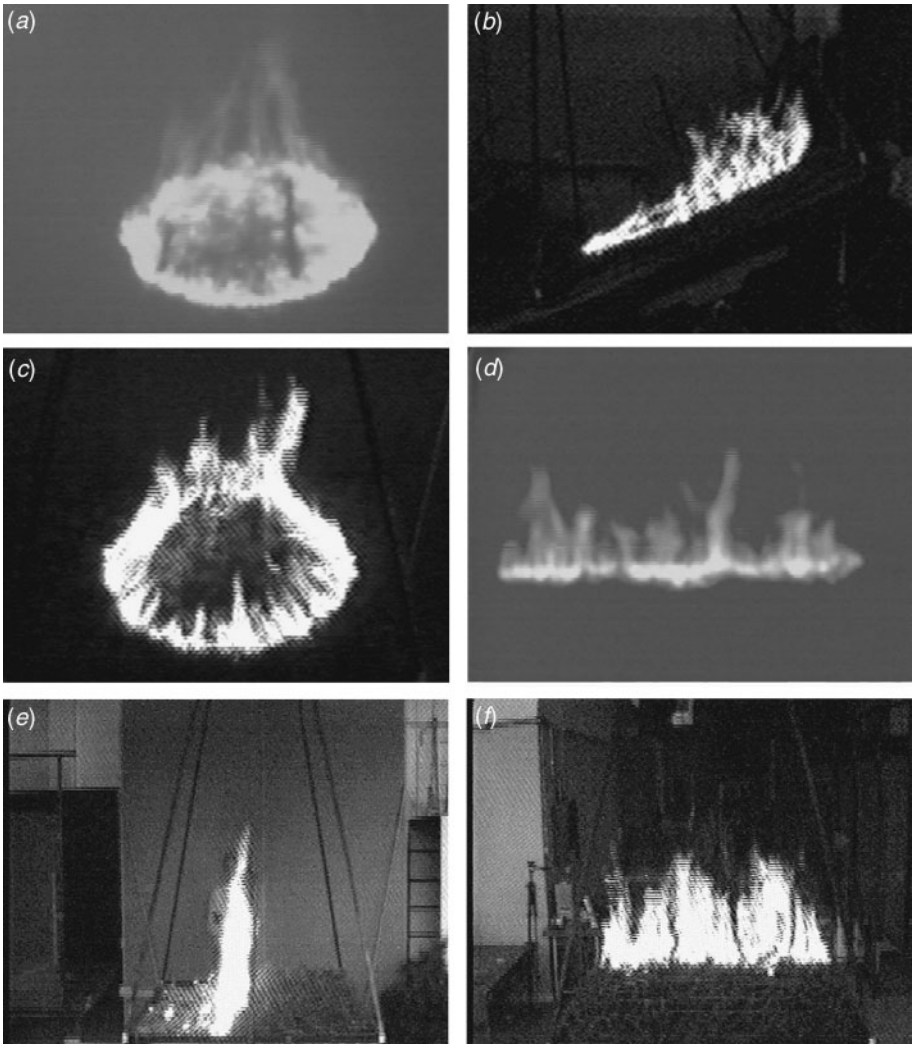

Fig. 2. Images obtained with infrared and visual cameras in frontal and lateral views in two fire experiments with point and linear ignitions. (*a*) Point, infrared (frontal); (*b*) point, visual (lateral); (*c*) point, visual (frontal); (*d*) linear, infrared (frontal); (*e*) linear, visual (lateral); (*f*) linear, visual (frontal).

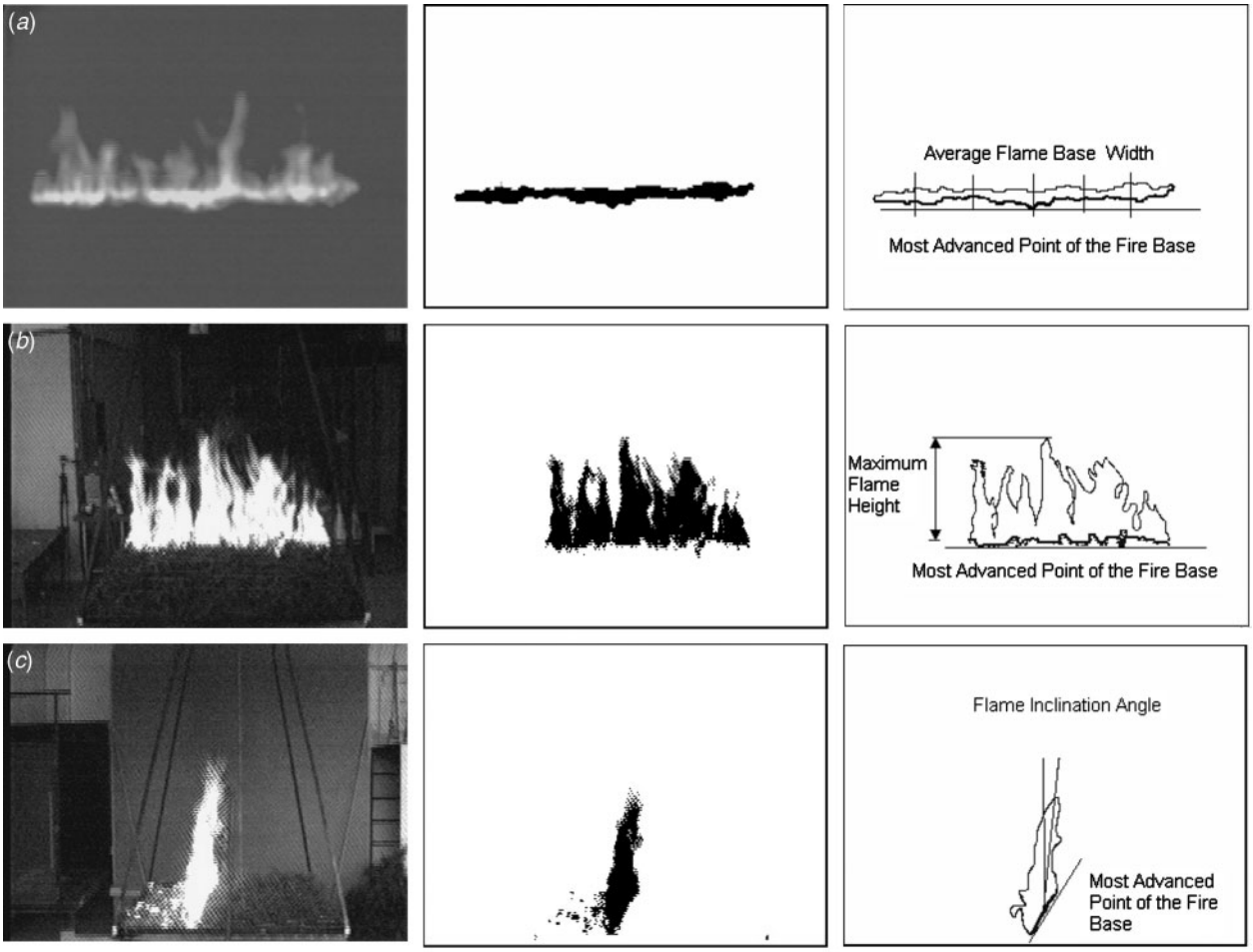

Fig. 3. Application of the basic set of image processing techniques to one infrared image (*a*) and two visual images (*b*,*c*), in a fire experiment with linear ignition. From left to right are represented: the original images, the images after differentiation of the fire from the background, and the final images.

estimations of temperature by using the emissivity indices of the materials in the scene and other physical parameters. For these cameras, a temperature threshold can be used to distinguish fire from background pixels. In order to avoid erroneous pixels in the fire borders, this temperature threshold should be selected taking into account the inaccuracies in the radiation–temperature conversion.

To facilitate the identification of the contour of the main fire front in the following step, a binary correction algorithm (Gonzalez and Woods 1992) was applied to eliminate spurious pixels with diverse origins, such as residual burning embers (see the central image of Fig. 3*c*), or flaming materials located beneath the top of the porous fuel bed, which appeared in the image when the burning table was inclined (see the central image of Fig. 3*b*).

Finally, to allow the automatic identification of the leading edge of the fire front, the observer must supply, at the configuration stage, the position of the camera (lateral or frontal) and the type of ignition (point or linear, the latter either at the bottom or at the top of the table).

Figure 3 illustrates the application of the above-mentioned techniques to three synchronous images of a fire experiment with linear ignition (left side of Fig. 3). Various geometrical features (expressed in image pixel coordinates) of the instantaneous fire front can now be measured in the final images (right side of Fig. 3), such as: the flame base width (Fig. 3*a*), the flame height (Fig. 3*b*), and the flame inclination angle (Fig. 3*c*).

Image calibration

The fire front measurements should now be converted from image pixel units into real-world length units through an appropriate image calibration technique. Two calibration techniques were used, whether the geometrical feature existed in a 2D plane (e.g. the leading edge of the fire front, which, in these experiments, lies in the surface of the fuel bed set upon the burn table) or in 3D space (e.g. the flame height). Note that the calibration process reduces to a trivial scaling transform (neglecting non-linear aberration effects of the optical system of the camera) only when the real object exists in

an object plane parallel to the image plane, with the optical axis of the camera perpendicular to the object plane. Even for plane objects, if the optical axis is oblique to the object plane, the image becomes non-linearly distorted and the attempt to reduce the calibration process to a simple scaling based on the average distance between the object plane and image plane leads to unacceptable errors.

The 2D calibration technique of Costa *et al*. (1998) was applied to flat real-world objects. It assumes that the camera has a pin-hole optical system without aberration. The object form, the position and orientation of the camera relative to the object, and the focal length of the camera are arbitrary and generally unknown. Four calibration points lying in the object plane at the vertices of a rectangle with known side lengths must be perceptible in the image. In infrared images, short candle flames were used as calibration points. Taking as input the pixel coordinates of a point on the image, the technique supplied as output the real-world coordinates of the corresponding point expressed in real-world units. The algorithm used was fully explicit and rather expeditious. An error analysis showed that the output had a systematic component of error mainly attributed to the calibration algorithm (including the identification of the calibration points in the image). There was also a random component of error mainly attributed to the identification of the point on the image. In the present analysis, the systematic (mean value) and random (standard deviation) components of error were both smaller than 0.5% of the real-world width of the image.

The 3D calibration technique of Tsai (1986) was also used. The internal (optical system) and external (position and orientation) calibration parameters were determined by an optimal fitting of the real-world coordinates of the calibration points through an iterative algorithm. The precision of the method increases with the number and accuracy of identifications of the calibration points in the image. The technique encompasses radial distortion in the image introduced by the optical system and is also designed to overcome lack of determination of the real-world coordinates of the object appearing in a single image by combining the information of multiple images provided by two or more cameras. In these experiments, the 3D calibration technique was only applied to visual cameras. The Tsai method was combined with the georeferencing method of Merino and Ollero (2002) to follow fire fronts propagating on general terrain surfaces described by a Digital Terrain Model (DTM).

Post-processing techniques for accuracy improvement and low-pass filtering

Consider a time sequence of measures of any fire features, $x(t_k)$ ($k = 0, 1, \ldots$), which results from the application of the former techniques to a sequence of images taken by one of the cameras. Superimposed on the physically meaningful trend of $x(t_k)$, there are random high-frequency fluctuations, 'random noise' in this context, with entangled origins, such as: high-frequency fluctuations of the fire front; noise in the images (e.g. smoke partially occluding the fire line edge in visual images); errors in the automatic measurement of geometrical features in pixel coordinates, and errors in the image calibration. To eliminate the random noise, two techniques were applied: Kalman filters, for measures obtained from a single camera, and sensor fusion techniques, for those estimated simultaneously from several cameras.

A 1D Kalman (1960) filter was applied to the measures of flame height, flame inclination angle, and fire front width. The parameters of the Kalman filter are the physical variance of the measure (q) and the measurement error variance (r). The values of these parameters for particular sequences of measures were estimated statistically. In the experiments, the values of q were observed to be systematically lower than the values of r. The values of r were also lower for measures obtained from infrared images than for measures obtained from visual images owing to the absence of smoke in the infrared images.

A feature-based data fusion technique was applied to the fire measures that were obtained from synchronous images of various cameras, such as flame height and position of the most advanced point. The data fusion procedure consists of a weighted average of the independent measures. The weights take into account the relative statistical confidence and spatial resolution of the cameras. This procedure shortens the width of the confidence interval of estimation of the true measure (Mohamad-Djafari 1997). Unfortunately, it cannot be applied to more complex features of the fire front, such as the shape of the fire front line.

3D representation

A simple 3D graphical representation model of the instantaneous fire front was constructed in real-time, based on measures of the fire front base (rear and leading edges position), and flame height and inclination angle. This graphical representation can be rendered from any point of view, simulating the image obtained by a virtual camera.

For instance, an experiment with a linear fire front spreading through a horizontal fuel bed was filmed with three synchronized cameras (Fig. 4*a*): an infrared frontal camera (*Camera 1*), and two visual cameras in lateral (*Camera 2*) and frontal (*Camera 3*) views. A 3D model of the fire front, 30 s after ignition, was constructed from the images of *Camera 1* and *Camera 2* (images are shown in Fig. 4*b*,*c*). This graphical representation is rendered as viewed by *Camera 3* in Fig. 4*d* (virtual image), and can be compared with the true image of *Camera 3* in Fig. 4*e*. For the whole test, the measures of maximum flame height based, independently, on the virtual view and on the real image, differed by a random magnitude with mean 2.3 mm and standard deviation 3.7 mm. Next, the images from the three cameras (combining their results with the sensor fusion technique) were used to construct a more accurate virtual view. As a consequence, the mean value and

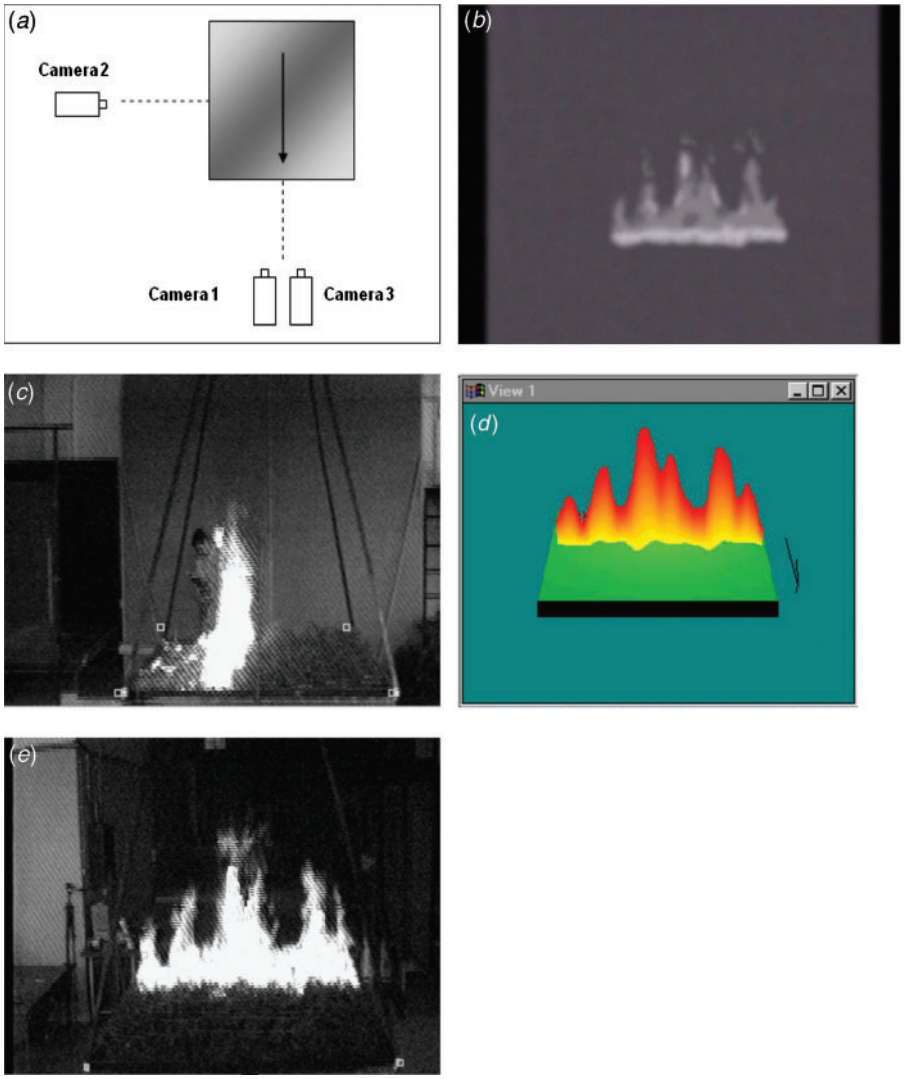

Fig. 4. Test with linear fire front, 30 s after ignition. (*a*) Camera configuration; (*b*) image of *Camera 1* (infrared, frontal); (*c*) image of *Camera 2* (visual, lateral); (*d*) 3D fire model based on the images of *Camera 1* and *Camera 2*, viewed by *Camera 3* (virtual image); and (*e*) true image of *Camera 3* (visual, frontal).

standard deviation of the former random error decreased to 0.9 mm and 1.8 mm, respectively.

Results

Figures 5 and 6 show the evolution of various properties of a linear fire front spreading up-slope (Fig. 5) and of a closed fire front point ignited (Fig. 6). In both cases, the slope angle was $\alpha = 20°$ and the measures were computed from the images of a frontal infrared camera and a lateral visual camera, using all the techniques presented above.

To illustrate the reliability of the method, Fig. 7 compares the measures of the position of the most advanced point of a linear fire front propagating down-slope obtained by this method (using only one frontal infrared camera) and by a manual method. The latter method is based on the measures taken with a manual chronometer of the time at which the fire front cut a sequence of threads previously stretched parallel to the ignition line and evenly spaced. The discrepancies between the measurements of both methods were always smaller than 1%.

Conclusions

The method presented in the present paper incorporates the following processing techniques:

(1) Techniques for image enhancement and fire contour detection: (i) median filter; (ii) method to distinguish fire from background for visual and infrared images; (iii) binary correction method; (iv) algorithm for fire

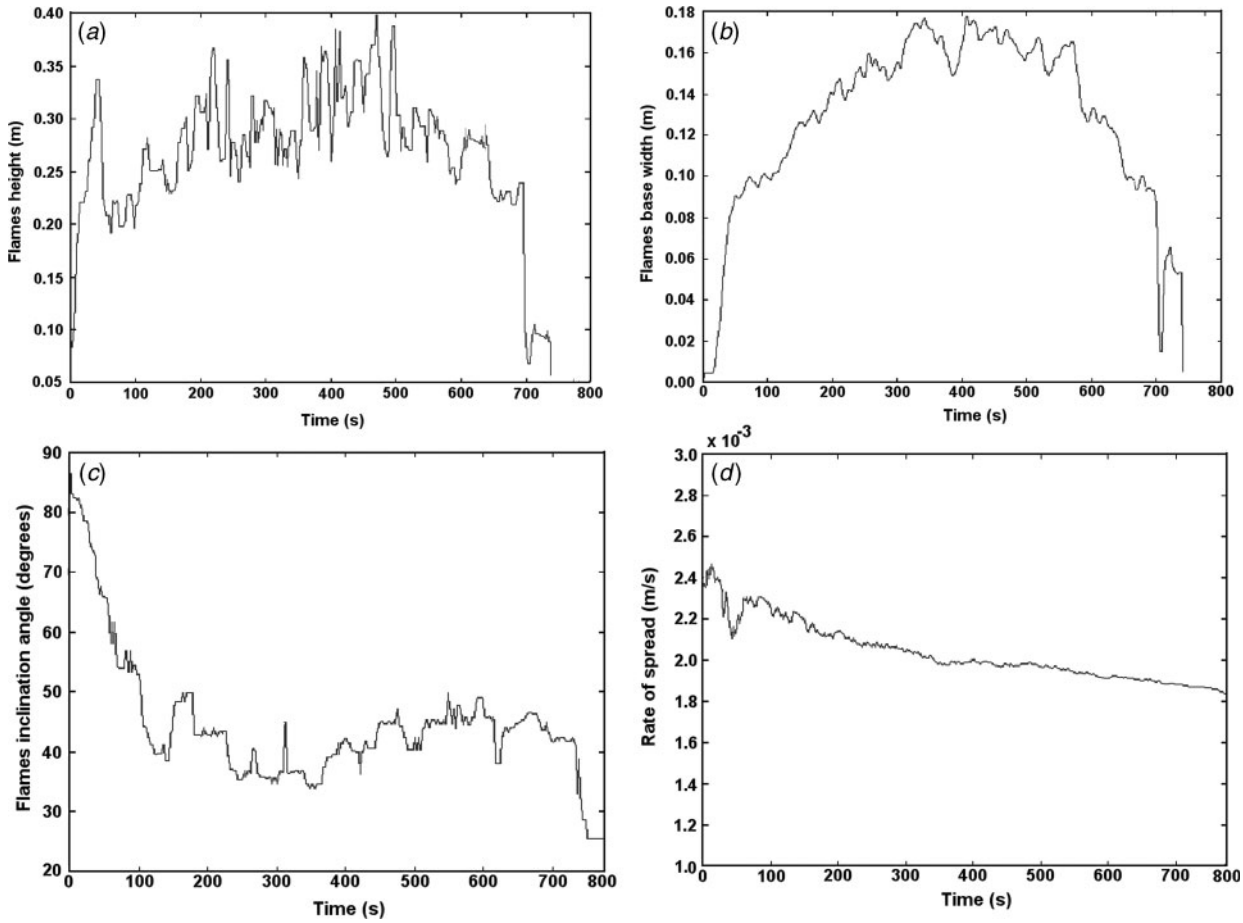

Fig. 5. Evolution of various properties of a linear fire front. (*a*) (Maximum) flame height; (*b*) (maximum) flame base width; (*c*) (average) value of flame inclination angle; and (*d*) rate of spread.

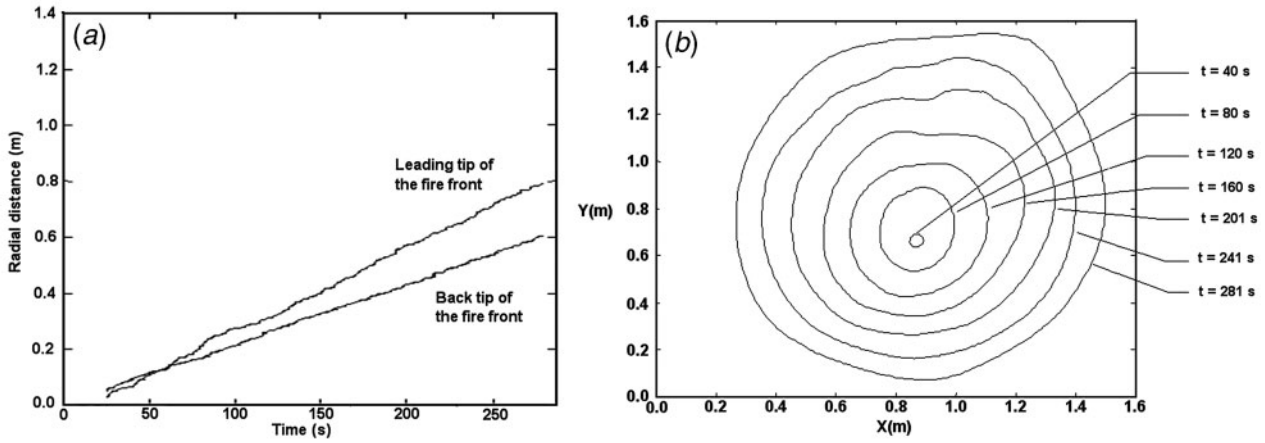

Fig. 6. Results obtained in a point ignition test. (*a*) Temporal evolution of the positions of the leading and rear tips of the fire front; and (*b*) fire front shape and position at several times during the test.

contour detection; and (v) methods for estimating various geometrical measures of the fire front in the image.

(2) Techniques for image calibration: (i) expeditious 2D technique, applicable only to measures on flat terrain; and (ii) 3D technique applied in all other cases.

(3) Post-processing techniques for improving the overall accuracy of the measures: (i) Kalman filters, for measures obtained from only one camera; and (ii) sensor fusion techniques for measures obtained from several cameras.

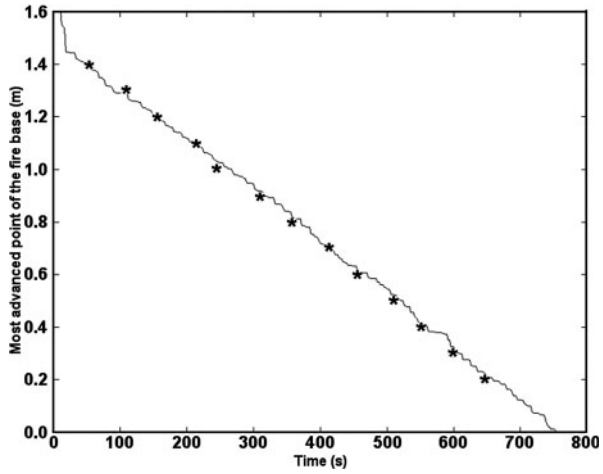

Fig. 7. Position of the most advanced point of a linear fire front propagating down-slope. Automatic (continuous line) *v.* manual (stars) methods.

(4) Technique of construction and rendering of a simple 3D graphical representation of the fire front.

To apply the method, the user needs:

(1) One or more static cameras (visual or infrared) viewing the whole burning table. A configuration allowing all measurements with reasonable accuracy consists of a frontal infrared camera and a lateral visual camera. The use of more synchronized cameras increases the accuracy of measurements. With only one camera it is not possible to measure some features of the fire front.
(2) A PC capable of importing the images and running the software implementing the techniques (e.g. a Pentium III at 600 MHz can run three-view tests in real-time).
(3) Marks (visible or hot points) at the four corners of the table or fuel bed, and a fully 3D grid, to calibrate visual and infrared images. Curved terrain surfaces should be described by a DTM.

The outputs and performance features of the method are the following:

(1) Primary output measures: fire front shape, position and width (fire front leading and rear edges), flame height and inclination angle. Secondary outputs: rate of spread, 3D representation of the fire front that can be rendered from any view.
(2) Time and space resolutions better than 1 s and 5 mm (conservative estimate; depends on the table dimensions and on the cameras). The method supplies the slowly varying instantaneous spatial distributions of most outputs, to which any type of space–time operators (e.g. average, maximum or minimum) can be applied.
(3) Fire fronts can be open or closed, with any shape. Terrain can be plane or curved (described by a DTM).
(4) Automatic real-time processing. The user is only asked to give some simple information on the experimental set-up at the configuration stage.
(5) Non-intrusive measurement procedure.
(6) Overall measurement errors depending on too many factors to be definable 'a priori'. However, the tests performed revealed that the method is, at least, as reliable as manual methods (in the few cases when the latter can be applied).

Although the method described in the present paper is directly aimed at, and is only demonstrated in laboratory experiments, it can also be extended to field applications (Viegas *et al*. 2002).

Acknowledgements

The authors express their gratitude to the European Commission (DG XII) for the support given through research projects INFLAME ('Fire Behaviour Prediction Modelling and Testing', Contract ENV4-CT98.0700) and SPREAD ('Forest Fire Prevention and Mitigation', Contract EVG1-CT-2001-00043), both funded by the Environment and Climate Program. The Spanish authors are also thankful to Francisco Rodriguez y Silva and Francisco Salas from the Forest Fire Prevention and Restoration Service of the Environment Service of Andalucía. The Portuguese authors add thanks to Luis Ribeiro and Nuno Luis for their help in the laboratory tests, and acknowledge the support given by the National Science Foundation through Project 34128/99.

References

Adkins CW (1995) 'Users' guide for fire image analysis system – Version 5.0: a tool for measuring fire behavior characteristics.' USDA Forest Service, Southern Research Station, General Technical Report SE-93. (Asheville, NC)

Britton CM, Karr BL, Sneva FA (1977) A technique for measuring rate of spread. *Journal of Range Management* **30**, 395–397.

Clark TL, Radke L, Coen J, Middleton D (1999) Analysis of small-scale convective dynamics in a crown fire using infrared video camera imagery. *Journal of Applied Meteorology* **38**, 1401–1420. doi:10.1175/1520-0450(1999)038<1401:AOSSCD>2.0.CO;2

Clements HB (1983) Measuring fire behaviour with photography. *Photogrammetric Engineering and Remote Sensing* **49**, 213–217.

Costa AM, Gonçalves JC, André JCS, Lopes AG, Viegas DX (1998) 'A technique to correct the perspective distortion of images of 2D-objects.' Deliverable of Project INFLAME. (ADAI, Mechanical Engineering Department, University of Coimbra: Coimbra)

Den Breejen E, Roos M, Schutte K, De Vries JS, Winkel H (1998) Infrared Measurements of Energy Release and Flame Temperatures of Forest Fires. In 'Proceedings of the 3rd International Conference on Forest Fire Research'. November 1998, Luso, Portugal. (Ed. DX Viegas) pp. 517–532. (ADAU, University of Coimbra: Portugal)

Gonzalez RC, Woods RE (1992) 'Digital image processing.' (Addison-Wesley: Reading, MA)

Hudson RD (1969) 'Infrared system engineering.' (John Wiley and Sons: New York)

Kalman RE (1960) A new approach to linear filtering and prediction problems. *Transactions of the ASME–Journal of Basic Engineering* **82**, 35–45.

Martínez-de Dios JR, Ollero A (2002) Automatic threshold selection for infrared images of fires. In 'Proceedings of the International Conference on Forest Fire Research'. November 2002, Luso, Portugal. (Ed. DX Viegas) (CD-ROM) (Millpress: Rotterdam)

Merino L, Ollero A (2002) Computer vision techniques for fire monitoring using aerial images. International Conference on Industrial Electronics, Control and Instrumentation – IECON 2002. 5–8 November 2002. (Ed. LG Franquelo) (CD-ROM) (IEEE Industrial Electronic Society: Piscataway, NJ)

Mohamad-Djafari A (1997) Probabilistic methods for data fusion. In 'Proceedings of the 17th International Workshop on Maximum Entropy and Bayesian Methods for Statistical Analysis'. August 1997, Boise, Idaho, USA. (Eds G Erickson, JT Rychert, CR Smith) (Kluwer Academic Publishers: Dordrecht, the Netherlands)

Ridler TW, Calvard S (1978) Picture thresholding using an iterative selection method. *IEEE Transactions on Systems, Man, and Cybernetics* **SMC-8**, 630–632.

Tsai RY (1987) Meteorology using off-the-shelf TV cameras and lenses. *IEEE Journal of Robotics and Automation* **3**, 323–344.

Viegas DX, Cruz MG, Ribeiro LM, Silva AJ, Ollero A, *et al*. (2002) Gestosa fire spread experiments. In 'Proceedings of IV International Conference on Forest Fire Research and 2002 Wildland and Fire Safety Summit'. (Ed. DX Viegas) (CD-ROM) (Millpress: Rotterdam)

Zhou X, Sun L, Weise D, Mahalingam S (2003) Thermal particle image velocity estimation for fire plume flow. *Combustion Science and Technology* **175**, 1293–1316.